Received 30 September 2018; revised 16 November 2018; accepted 21 November 2018. Date of publication 27 November 2018;
date of current version 1 March 2019. The review of this paper was arranged by Editor C. C. McAndrew.

Digital Object Identifier 10.1109/JEDS.2018.2883585

A New High-Gain Operational Amplifier Using Transconductance-Enhancement Topology Integrated With Metal Oxide TFTs

ZHUO-JIA CHEN [1], WEN-XING XU [1], JIAN-DONG WU [1], LEI ZHOU [2], WEI-JING WU [3] (Member, IEEE), JIAN-HUA ZOU [2], MIAO XU [3], LEI WANG [3], YU-RONG LIU [1], AND JUN-BIAO PENG [3]

1 School of Electronic and Information Engineering, South China University of Technology, Guangzhou 510640, China
2 Research and Development Department of New Vision Opto-Electronic Technology Company, Ltd., Guangzhou 510530, China
3 State Key Laboratory of Luminescent Materials and Devices, South China University of Technology, Guangzhou 510640, China

CORRESPONDING AUTHOR: W.-J. WU (e-mail: wuwj@scut.edu.cn)

This work was supported in part by the National Key Research and Development Program of China under Grant 2016YFB0401005, in part by 973 Program funded by the Ministry of Science and Technology under Grant 2015CB655004, in part by the National Natural Science Foundation of China under Grant 61874046, Grant 61871195, Grant 61574062, and Grant 61574061, in part by the Science and Technology Program of Guangdong Province under Grant 2016B090906002, Grant 2017B090901055, Grant 2017B090901006, and Grant 2017B090907016, in part by the International Cooperation Program of Guangzhou Economic and Technological Development Zone under Grant 2017GH29, and in part by the Fundamental Research Funds for the Central Universities under Grant 2017ZD059.

ABSTRACT This paper presents an integrated operational amplifier (OPAMP) consisting of only n-type metal oxide thin-film transistors. In addition to using positive feedback in the input differential pair, a transconductance-enhancement topology is applied to improve the gain of the OPAMP. The OPAMP has a voltage gain (A_v) of 29.54 dB over a 3-dB bandwidth of 9.33 kHz at a supply voltage of 15 V. The unity-gain frequency, phase margin (PM), and dc power consumption (P_{DC}) are 180.2 kHz, 21.5° PM and 5.07 mW, respectively.

INDEX TERMS Operational amplifier, transconductance-enhancement topology, positive feedback, metal oxide thin-film transistors (TFTs).

I. INTRODUCTION

Metal oxide thin-film-transistors (TFTs) are believed to be a promising technology in main large area electronics technologies due to the advantages of higher mobility compared with a-Si:H TFTs, good uniformity and low-temperature fabrication compared with LTPS TFTs [1]–[3]. In recent years, there has been increasing interest in applying oxide-based TFTs to integrated circuits (ICs), such as display drivers, converters or RFID/NFC tags [4]–[6]. In addition, they also have a potential interesting application in the bio-potential monitoring system [7], [8]. Among them, the operational amplifier is the most important module used to amplify signals in analog circuits. However, there are various design challenges for metal oxide TFTs realizing operational amplifiers, as only N-type TFTs are available for integration. First, the transconductance of metal oxide TFTs is not high enough because the electrical mobility of metal oxides is much lower than that of crystalline silicon [9]. Second, it is difficult to obtain high output impedance in amplifier design due to the lack of a p-type TFT. Some operational amplifiers based on metal oxide TFTs have been reported in recent years [1], [10], [12]. In [1] and [10], positive feedback and pseudo-CMOS technology were presented to boost the output impedance of an operational amplifier. Two-stage Cherry-Hooper topology has also been used to increase the voltage gain and gain-bandwidth product (GBWP) of amplifiers based on metal oxide TFTs [11]. In addition, compensating for the threshold voltage shift of n-type TFTs can increase the phase margin to improve stability [12]. In fact, the gain of an amplifier can also be increased if the equivalent transconductance of the amplifier is improved.

This paper proposes a new differential amplifier with high gain integrated by metal oxide thin-film-transistors. A transconductance-enhancement topology is used to boost the equivalent transconductance of the amplifier. And, positive feedback is applied to obtain a high output impedance.

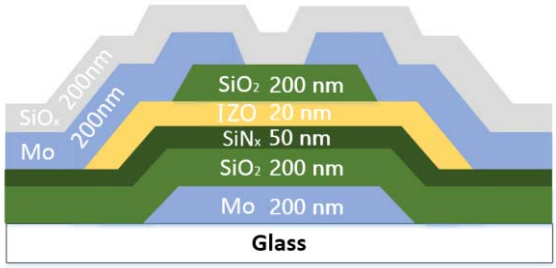

FIGURE 1. Structure of metal oxide TFT.

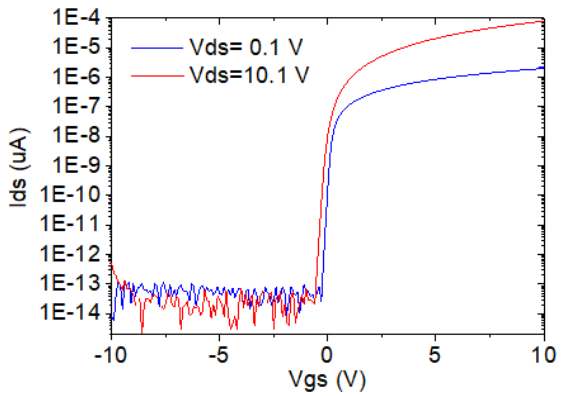

FIGURE 2. Transfer characteristics of the TFT with W/L = 30 μm/10 μm.

II. PROCESS TECHNOLOGY

Fig. 1 shows the etch-stop layer (ESL) structure of the IZO TFTs integrated into the proposed operational amplifier. The fabrication process is described as follows. A 200-nm molybdenum (Mo) layer is deposited onto a glass substrate as the gate electrode via DC sputtering and patterned via wet etching. Then, 250-nm SiO_2 and 50-nm SiN_x are successively deposited by plasma-enhanced chemical vapor deposition (PECVD) as stacked insulator layers and patterned by dry etching. A 20-nm IZO active layer is deposited on the insulator by RF magnetron sputtering. Afterwards that, a 200-nm SiO_2 is deposited by PECVD at 230 °C as the etch-stop layer. Subsequently, 200-nm Mo is sputtered as the source and drain electrodes. Finally, a 200-nm thick SiO_x layer is deposited by PECVD at 350 °C to protect the device.

Fig. 2 shows the measured transfer characteristics of the TFTs with W/L = 30 um/10 um at $V_{ds} = 0.1$ V and 10 V. The threshold voltage, the field-effect mobility and the subthreshold swing are extracted as 1.0 V, 33 cm^2/ (V s) and 0.11 V/dec, respectively.

III. CIRCUIT DESIGN

Two major effect factors of the operational amplifier (OPAMP) voltage gain are the input transconductance (G_m) and its effective load resistance (R_L). The small-signal equivalent voltage gain can be given by

$$A_v = -G_m \times R_L \tag{1}$$

Therefore, it is necessary to increase G_m and R_L to boost the OPAMP small-signal voltage gain. In the absence of p-type TFTs, positive feedback circuits are normally used to increase G_m and R_L in an amplifier integrated with n-type TFTs [1], [13].

A. POSITIVE FEEDBACK

Fig. 3 (a) shows a common-source amplifier topology with positive feedback, which has already been implemented in IGZO technology [12], [14]. And it is made up of a single-ended common-source TFT (T_1), a load TFT (T_2) and a feedback amplifier (A_f). The voltage gain of this circuit can be expressed as

$$A_v = \frac{\partial V_{out}}{\partial V_{in}} = -g_{m1}\left[\frac{1}{g_{m2}(1-A_f)}||r_{01}||r_{02}\right] \tag{2}$$

where A_f is a positive feedback factor, which can be achieved by cascading two common-source amplifiers as shown in Fig. 3. (b). This can be expressed as

$$A_f = \frac{\partial V_F}{\partial V_o} = \frac{g_{m1}g_{m3}}{(g_{m2}||r_{02})(g_{m4}||r_{04})} \approx \frac{g_{m1}g_{m3}}{g_{m2}g_{m4}} \tag{3}$$

It is assumed that all the TFTs in Fig. 3 (b) operate in the saturation region and their DC currents are same, meaning that the feedback amplifier gain can also be given by

$$A_f \approx \frac{g_{m1}g_{m3}}{g_{m2}g_{m4}} = \frac{\sqrt{(W/L)_1}\sqrt{(W/L)_3}}{\sqrt{(W/L)_2}\sqrt{(W/L)_4}} \tag{4}$$

Consequently, the voltage gain of a common-source amplifier with positive feedback can be controlled by the ratio of the channel width to channel length. In fact, this circuit mainly increases the amplifier voltage gain by increasing its effective load resistance (R_L). As the feedback circuit has a gain of unity, the effective load resistance is approximately equal to r_{02}. Therefore, the voltage gain is boosted to a value of g_{m1} ($r_{01} \| r_{02}$), which can be extracted by (2) and is close to the intrinsic gain of NTFTs. Therefore, n-type TFT amplifier gain enhancement can be achieved by varying the feedback circuit gain from zero to one ($0 < A_f < 1$). For a common-source amplifier with a feedback gain larger than unity, a shunt negative resistance is equivalently provided by the load, making it possible to further boost the voltage gain at the cost of circuit stability. In this positive feedback technique, a feedback circuit gain slightly smaller than unity is adopted as the design goal to ensure circuit stability, even in the presence of process variations [1].

B. TRANSCONDUCTANCE-ENHANCEMENT TOPOLOGY

In fact, feedback circuits can not only improve the stability and load configuration of an operational amplifier, but also be used to change the transconductance of the amplifier. In some applications, a resistor is placed in series with the source terminal of the transistors to attenuate the square-law dependence of the drain current on the overdrive voltage, as depicted in Fig. 4. (a). Here, the drain current (i_{out}) and the voltage drop across R_s increase with increasing v_{in}. That is,

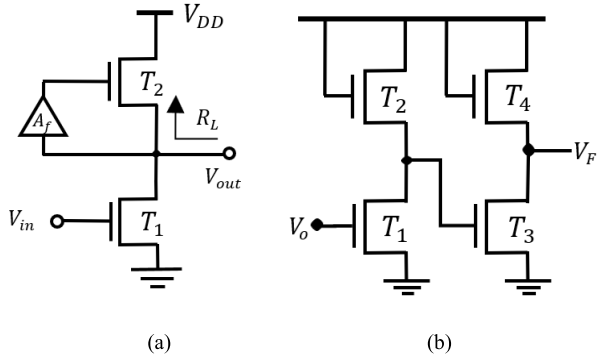

FIGURE 3. **(a) Common-source amplifier topology with positive feedback, (b) A feedback amplifier (A_f), where V_F is the feedback voltage.**

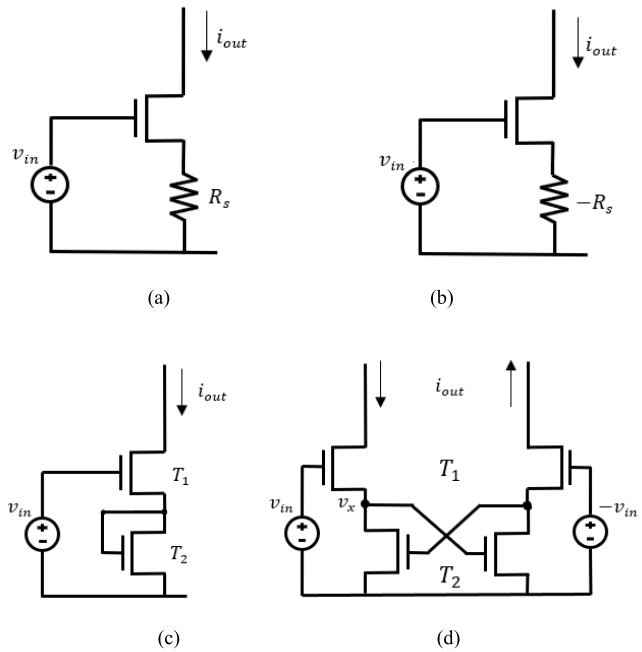

FIGURE 4. **Optimized input transconductance topology for operational amplifiers (a) driving TFT with source degeneration (negative feedback). (b) Driving TFT with source improvement (positive feedback). (c) Driving TFT with a diode-connected device in source. (d) Transconductance enhancement realized in the different form.**

a fraction of v_{in} appears across the resistor, thus leading to a decrease in the transconductance. Similarly, the transconductance of the amplifier is increased by placing a "negative" resistor in series with source terminal, as shown in Fig. 4 (b). Essentially, a positive feedback system is added to the driving TFT to enhance the transconductance of this circuit. The equivalent transconductance can be expressed as

$$G_m = \frac{g_m}{1 - g_m R_s} \tag{5}$$

where $g_m R_s$ is less than 1.

A resistor with a precise value and a reasonable physical size is difficult to be fabricated by the TFTs process. Consequently, it is desirable to replace R_s with a "diode-connected" TFT, as shown in Fig. 4. (c). A "negative" resistor can be easily realized by a differential form, as shown in Fig. 4. (d). Based on small signal analysis, the drain current (i_{out}) increases, but v_x decreases with an increase in the amplitude of v_{in}. Therefore, the gate-source overdrive voltage of T_1 and the equivalent transconductance increase. Neglecting the channel-length modulation for simplicity, the equivalent transconductance of this circuit is given by

$$G_m = \frac{g_{m1}}{1 - \frac{g_{m1}}{g_{m2}}} \tag{6}$$

where g_{m1} and g_{m2} are the transconductances of transistors T_1 and T_2, respectively. Due to the symmetric structure, both sides of this circuit carry equal DC currents and G_m values. The ratio of g_{m1} to g_{m2} can be determined accurately since this value is the square root of the ratio of $(W/L)_1$ to $(W/L)_2$. In addition, this transconductance-enhancement topology increases transconductance of the amplifier by introducing positive feedback in the case of differential mode input. However, this topology is a common-source stage with source degeneration in the case of common mode input. It means that this topology can also improve linearity of the OPAMP and reduce dc current.

Fig. 5 shows two different transconductance-enhancement topologies of the differential amplifier with diode-connected load. In fig. 5 (a), two double gate devices are connected as a source couple differential pair to create a positive feedback for increasing the gain [7]. And this amplifier topology has a similar gain equation to fig. 5 (b). However, there are two aspects to consider about this double-gate based topology. On the one hand, it is hard to select the bias point for the device working at the saturation region because the top gate of the device is connected to the output. On the other hand, the linearity of the OPAMP is reduced due to the positive feedback introduced in the topology.

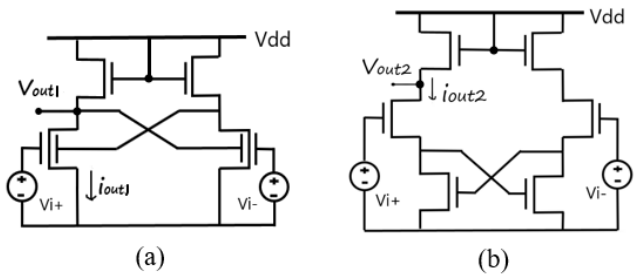

FIGURE 5. **Schematic of two differential amplifiers with diode-connected load. (a) Double gate TFTs based transconductance enhancement topology of [7]. (b) Transconductance-enhancement topology of this work.**

C. PROPOSED OPAMP

Fig. 6 presents the schematic of the proposed OPAMP with the dimensions of each transistor, which consists of only n-type TFTs. This circuit can be divided into two stages. The first stage includes a differential input circuit (T_1-T_5) with a transconductance-enhancement topology (T_6, T_7) and

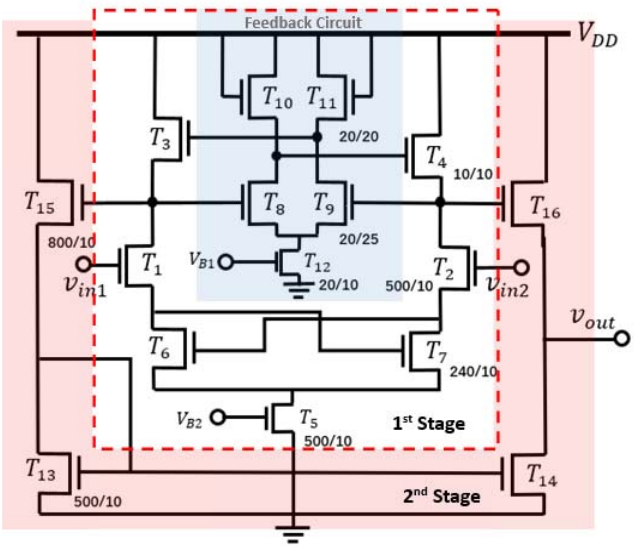

FIGURE 6. Schematic of the proposed high gain amplifier with positive feedback.

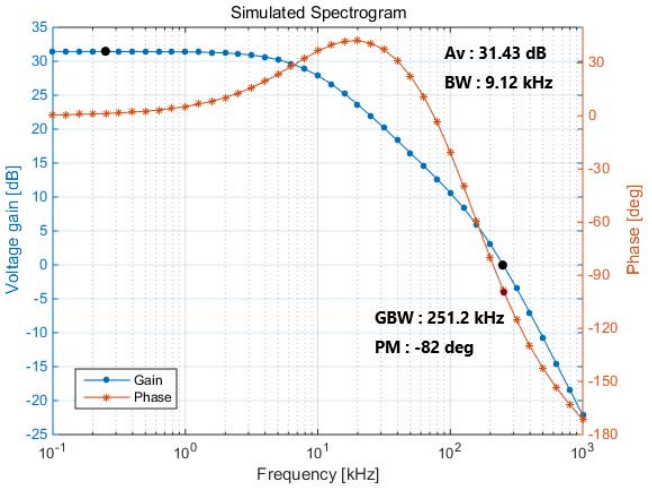

FIGURE 7. Simulated frequency response of the proposed OPAMP.

a positive feedback circuit (T_8-T_{12}) for obtaining the effective load resistance. All the TFTs of this OPAMP work in the saturation region by adjusting the bias voltage $V_{B1,2}$. In the second stage, a differential-to-single-ended converter composed of T_{13}-T_{16} is utilized as the output buffer [15]. To maintain a constant gain, the differential-to-single-ended converter requires a stable tail current source, which can be achieved by a current mirror circuit. The calculated gains of each stage are given by

$$A_{1st} = \frac{g_{m1}}{1-\frac{g_{m1}}{g_{m6}}}\left(\frac{1}{g_{m3}(1-A_f)}\|r_{03}\|r_{01}\right) \tag{7}$$

$$A_{2nd} = g_{m16}\left(\frac{1}{g_{m16}}\|r_{016}\|r_{014}\right) \tag{8}$$

where

$$A_f = g_{m8}\left(\frac{1}{g_{m10}}\|r_{08}\|r_{010}\right) \approx \frac{g_{m8}}{g_{m10}} \tag{9}$$

consequently, the overall voltage gain of this proposed operational amplifier can be given by

$$A_v = \frac{g_{m1}}{1\frac{g_{m1}}{g_{m6}}}\left(\frac{1}{g_{m3}(1-A_f)}\|r_{03}\|r_{01}\right)g_{m16}\left(\frac{1}{g_{m16}}\|r_{016}\|r_{014}\right) \tag{10}$$

when A_f is close to one, A_v can be reduced to

$$A_v \approx \frac{g_{m1}}{1-\frac{g_{m1}}{g_{m6}}}(r_{03}\|r_{01}) \tag{11}$$

where g_{m1} and g_{m6} are the transconductances of the transistors of T_1 and T_6, respectively, and r_{01} and r_{03} are the output resistances of T_1 and T_3, respectively. The overall voltage gain is mainly determined by the first stage, where the gain can be improved by increasing the ratio of g_{m1} to g_{m6}, or by adjusting the bias voltage (V_{B2}) to increase r_{01} and r_{03}.

Note that, two positive feedback loops in the proposed OPAMP may increase the possibility of instability although they are used to increase the gain. As a result, it is important to keep the positive feedback gain (A_f and gm1/gm6) sufficiently smaller than one. The dominant poles are located at the output node of the input stage. For achieving sufficient phase margin, TFTs with large aspect ratios are employed in the second stage to move the secondary poles toward higher frequencies [1]. The design of the proposed OPAMP is verified by the SMART-SPICE software, in which the RPI poly-Si TFT model (level 36) is used to fit the characteristic of metal oxide TFTs. Then, the size of each TFT is carefully determined through the simulation results for achieving high gain while ensuring the OPAMP stability. And the dimensions of all TFTs are indicated in Fig. 6.

Fig. 7 shows the simulated frequency response of the proposed OPAMP. The simulated voltage gain, bandwidth, unity-gain frequency and phase margin are 31.43 dB, 9.12 kHz, 251.2 kHz and −82°, respectively. Note that, the transconductance-enhancement topology produces a zero closer to the origin, which causes the rising of the phase and the degradation of the stability. Therefore, it is important to choose the appropriate aspect ratios of TFTs to balance the impacts of zero and pole on the stability of the OPAMP.

IV. EXPERIMENTAL RESULTS

The proposed OPAMP was successfully implemented on a glass substrate using metal oxide TFT manufacturing technology. Fig. 8 shows a microphotograph of the proposed OPAMP, where the dimensions of the circuit and input-output interfaces are denoted. In order to reduce the V_{TH} mismatch of the differential pair transistors (T1/T2 and T8/T9), symmetry design and multiple fingers design were used in the circuit layout. An oscilloscope (DSO-X 4014A), a signal generator (NF WF1948) and a semiconductor parameter analyzer (Agilent B1500A) were used to measure this

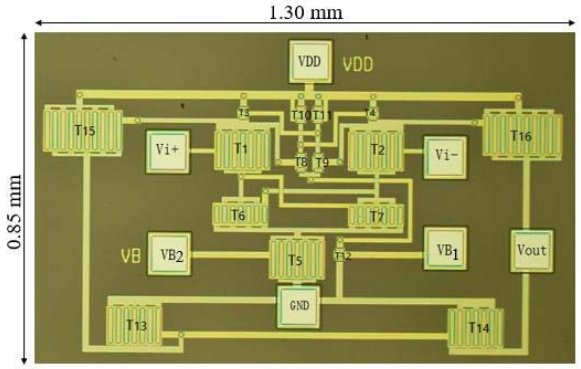

FIGURE 8. Microphotograph of the proposed operational amplifier.

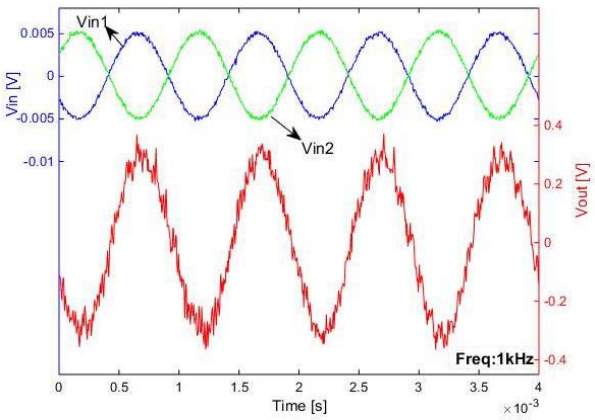

FIGURE 9. Measured input and output waveforms of the proposed OPAMP with 10 mVpp and1 kHz sinusoid differential input.

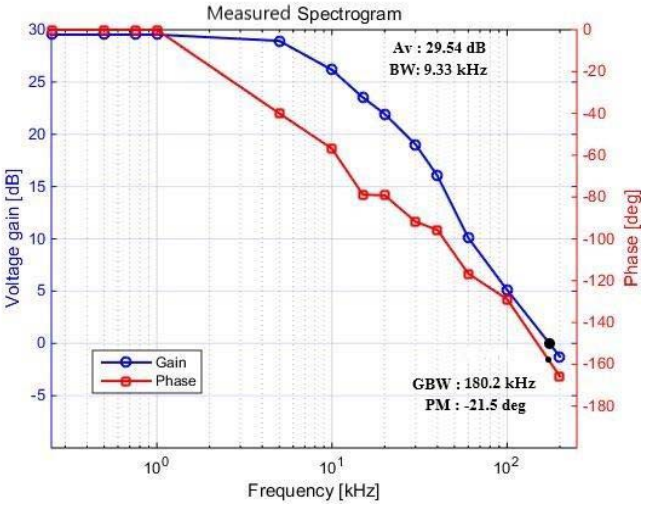

FIGURE 10. Measured frequency response of the proposed OPAMP.

OPAMP under normal room temperature and daylight conditions. The measurements of the circuit were carried out with 15 V DC supply-voltage. Both V_{B1} and V_{B2} were provided with an external voltage source of which the value was 1.5 V. Fig. 9 shows the measured input and output waveforms of the proposed OPAMP with a sinusoidal differential input of 1 kHz, 10 mVpp (peak to peak) and 3.5 V dc bias. The measured voltage gain and phase are 29.54 dB [$G_m = 20\ lg\ (V_{out}/(V_{i+}\text{-}V_{i-}))$] and zero degrees [$\varphi_m = \varphi_{Vout} - \varphi_{Vi+}$)], respectively. As seen from Fig. 9, the output signal looks noisy due to the noise in the input signal originating from the ground wire.

Fig. 10 shows the measured frequency response of the proposed OPAMP based on metal oxide TFTs. The voltage gain is 29.54 dB, and the unity-gain frequency is 180.2 kHz with 21.5° PM (phase margin). The measured 3 dB bandwidth (BW) is 9.33 kHz, and the gain-bandwidth-product (GBWP) is calculated to be 279.9 kHz. Compared with fig. 7, the gain and 3 dB bandwidth are close to the simulated results, while the phase margin and unity-gain frequency are significantly smaller for the measured results. That is perhaps because the parasitic capacitance and V_{TH} variation cause the position of the zero and the secondary pole shifting. Especially, the effect of the zero closer to the origin is not obviously detected in the measured frequency response. It might be because the layout parasitic capacitance existing next to T1 and T2 weakens the effect of zero.

In addition, amplifiers with feedback systems may suffer from instability problems. According to Fig. 10, the gain margin (G_m) and phase margin (φ_m) of this OPAMP are −3.71 dB and 21.5 degrees, respectively. In Fig. 10, the OPAMP was appears to be a stable system since the gain crossover occurs before the phase crossover. However, it is usually required that $G_m \leq -10$ dB, or $\varphi_m = 45°\sim60°$ in industrial practice. The phase margin can be increased by using frequency compensation to avoid the existence of mirror poles in a differential-to-single circuit, or compensating V_{TH} variations in the TFTs [12].

TABLE 1 summarizes the OPAMP performances and provides a comparison with other metal oxide TFT amplifier designs reported in the literature. The voltage gain of the proposed OPAMP is higher than those of all other designs, except [7]. The OPAMP in [7] used fully differential operational amplifier structure of which the gain is generally bigger than the differential operational amplifier with differential-to-single-ended converter. Compared with other designs, the proposed OPAMP only uses one stage to achieve high gain, in which the second stage is just a differential-to-single-ended converter without the function of increasing the gain. In addition, the GBWP and unit-gain frequency seem relatively high. Without the influence of the mirror pole and positive feedback, the GBWP of the OPAMP with a smaller power supply in [16] is about 5 times that of this work. Of courses, the self-aligned process technology may also help to improve GBWP [17]. As result, the transconductance-enhancement topology connecting a "negative" resistor to the source terminal of the driving TFT can increase the voltage gain of the operational amplifiers.

TABLE 1. Comparison of differential amplifier in metal oxide TFT.

Circuit	[4]	[16]	[10]	[12]	[7]	This work
Topology	NMOS diode		Pseudo-CMOS	Positive feedback		
VDD [V]	±15	5	5	6	±10	15
A_V [dB]	24.5	18.7	22.5	19	30	29.54
BW [kHz]	6	108	5.6	25	0.15	9.33
GBWP [kHz]	101.9	930	74.7	223	4.74	279.9
Unit-gain Frequency [kHz]	32	472	31	330	5.5	180.2
PM [Deg.]	NA	NA	≈-15	-70	NA	-21.5
P_{DC} [mW]	NA	0.9	0.16	6.78	0.19	5.07
Nr. of amplification stages	3	3	2	1	1	1

However, this circuit does not provide a sufficient phase margin compared with those in previous works because of the mirror pole of differential-to-single-ended converter and the zero of transconductance-enhancement topology. Note that, the threshold voltage compensation technique can also be used to increase the phase margin of the OPAMP, which has been reported in [12].

V. CONCLUSION

This work presents the design and characterization of a new operational amplifier integrated by metal oxide TFTs. The proposed OPAMP consists of a differential input stage and a differential-to-single ended stage. Two strategies were applied to improve the gain: positive feedback and a transconductance-enhancement topology. The measured voltage gain of the OPAMP is as much as 29.54 dB compared with that of other amplifiers integrated by metal oxide TFTs. The measured bandwidth, unity-gain frequency, and DC power consumption are 9.33 kHz, 180.2 kHz and 5.07 mW, respectively. As a result, this proposed OPAMP with high gain and sufficient bandwidth may be used to amply sensing signals, such as bio-potential signals or optical signals.

REFERENCES

[1] Y.-C. Tarn, P.-C. Ku, H.-H. Hsieh, and L.-H. Lu, "An amorphous-silicon operational amplifier and its application to a 4-bit digital-to-analog converter," *IEEE J. Solid-State Circuit*, vol. 45, no. 5, pp. 1028–1035, May 2010.
[2] J. H. Lee *et al.*, "World's largest (15-inch) XGA AMLCD panel using IGZO oxide TFT," in *SID Symp. Dig. Tech. Papers*, vol. 39, May 2008, pp. 625–628.
[3] S. Xiaofeng *et al.*, "A new poly-Si TFT compensation pixel circuit employing AC driving mode for AMOLED displays," *J. Semicond.*, vol. 34, no. 12, Dec. 2013, Art. no. 125011.
[4] K. Kim, K.-Y. Choi, and H. Lee, "A-InGaZnO thin-film transistor-based operational amplifier for an adaptive DC–DC converter in display driving systems," *IEEE Trans. Electron Devices*, vol. 62, no. 4, pp. 1189–1194, Apr. 2015.
[5] Z.-W. Zong *et al.*, "A new surface potential-based compact model for a-IGZO TFTs in RFID applications," in *Proc. IEEE Int. Electron Devices Meeting*, Dec. 2012, pp. 35.5.1–35.5.4.
[6] K. Myny *et al.*, "16.3 Flexible thin-film NFC tags powered by commercial USB reader device at 13.56MHz," in *Proc. IEEE Int. Solid-State Circuits Conf.*, Feb. 2015, pp. 1–3.
[7] C. Garripoli *et al.*, "Analogue frontend amplifiers for bio-potential measurements manufactured with a-IGZO TFTs on flexible substrate," *IEEE J. Emerg. Sel. Topics Circuits Syst.*, vol. 7, no. 1, pp. 60–70, Mar. 2017.
[8] T. Sekitani *et al.*, "Stretchable electrons for wearable microvolt bio-signal monitoring systems," in *SID Symp. Dig. Tech. Papers*, vol. 49, pp. 84–86, May 2018.
[9] P. G. Bahubalindruni, V. Tavares, P. B. Barquinha, R. Martins, and E. Fortunato, "Basic analog and digital circuits with a-IGZO TFTs," in *Proc. IEEE Int. Conf. Synth. Model. Anal. Simulat. Methods Appl. Circuit Design*, Jun. 2016, pp. 1–4.
[10] K. Ishida *et al.*, "22.5 dB open-loop gain, 31 kHz GBW Pseudo-CMOS based operational amplifier with a-IGZO TFTs on a flexible film," in *Proc. IEEE Asian Solid-State Circuits Conf.*, Nov. 2014, pp. 313–316.
[11] R. Shabanpour *et al.*, "Cherry-Hooper amplifiers with 33 dB gain at 400 kHz BW and 10 dB gain at 3.5 MHz BW in flexible self-aligned a-IGZO TFT technology," in *Proc. IEEE Int. Symp. Intell. Signal Process. Commun. Syst.*, Dec. 2014, pp. 1–4.
[12] R. Shabanpour *et al.*, "A 70°phase margin OPAMP with positive feedback in flexible a-IGZO TFT technology," in *Proc. IEEE 58th Int. Midwest Symp. Circuits Syst.*, Oct. 2015, pp. 1–4.
[13] S. Sambandan, "High-gain amplifiers with amorphous-silicon thin-film transistors," *IEEE Electron Device Lett.*, vol. 29, no. 8, pp. 882–884, Aug. 2008.
[14] C. Garripoli *et al.*, "15.3 An a-IGZO asynchronous delta-sigma modulator on foil achieving up to 43dB SNR and 40dB SNDR in 300Hz bandwidth," in *Proc. IEEE Int. Solid-State Circuits Conf. (ISSCC)*, San Francisco, CA, USA, 2017, pp. 260–261.
[15] Y. P. Tsividis and P. R. Gray, "An integrated NMOS operational amplifier with internal compensation," *IEEE J. Solid-State Circuit*, vol. SC-11, no. 6, pp. 748–753, Dec. 1976.
[16] C. Zysset *et al.*, "IGZO TFT-based all-enhancement operational amplifier bent to a radius of 5 mm," *IEEE Electron Device Lett.*, vol. 34, no. 11, pp. 1394–1396, Nov. 2013.
[17] R. Shabanpour *et al.*, "High gain amplifiers in flexible self-aligned a-IGZO thin-film-transistor technology," in *Proc. IEEE Int. Conf. Electron. Circuits Syst.*, Dec. 2014, pp. 108–111.

ZHUO-JIA CHEN is currently pursuing the master's degree in integrated circuit engineering with the School of Electronic and Information Technology, Guangzhou, China.

Her current research interests include design of analog integrated circuits by thin film transistors.

WEN-XING XU is currently pursuing the master's degree in integrated circuit engineering with the School of Electronic and Information Technology, Guangzhou, China.

His research interests include integrated circuits by thin film transistors.

JIAN-DONG WU received the M.S. degree in integrated circuit engineering from the South China University of Technology, Guangzhou, China, in 2018.

In 2018, he joined Shenzhen State Microelectronics Company, Ltd, Shenzhen, where he is involved in analog integrated circuits design. His current research interests include the design of PLL and LDO.

LEI ZHOU was born in China in 1987. He received the B.Sc. degree in microelectronics and the M.Sc. degree in microelectronics and solid-state electronics from the South China University of Technology, Guangzhou, China, in 2010 and 2013, respectively.

In 2013, he joined Guangzhou New Vision Optoelectronic, Guangzhou, where he is involved in AMOLED display panel design. His current research interests include pixel design, ESD design, and touch sensor based on metal-oxide thin-film transistors.

WEI-JING WU (M'09) was born in Fuzhou, China. He received the Ph.D. degree from the South China University of Technology, Guangzhou, China, in 2008.

In 2008, he joined the Institute of Polymer Optoelectronic Materials and Devices, South China University of Technology, where he is currently an Associate Professor with the State Key Laboratory of Luminescent Materials and Devices. His current research interests include thin-film transistors circuits and AMOLED displays.

JIAN-HUA ZOU received the bachelor's degree in materials physics from North East University, China, in 2005 and the Ph.D. degree from the Physics Department, South China University of Technology, China, in 2010.

In 2018, he joined Guangzhou New Vision Optoelectronic Technology Company, Ltd. His current research interests are organic electronics and optoelectronics, including LEDs, thin film transistors, and organic photoelectric detection. He has published over 50 papers on high-impact journals in the above areas.

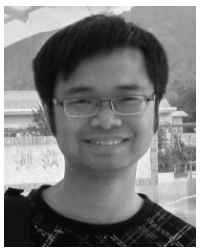

MIAO XU was born in China in 1982. He received the B.Sc. degree in applied physics and the M.Sc. degree in condensed matter physics from the Harbin Institution of Technology, Harbin, China, in 2004 and 2007, respectively, and the Ph.D. degree in materials physics and chemistry from the South China University of Technology, Guangzhou, China, in 2010.

He was with the School of Electronic and Information Engineering, South China University of Technology. His current research interests include metal-oxide thin-film transistors and flexible electronics devices.

LEI WANG received the B.Sc. degree in polymer materials science and engineering from the Hebei University of Technology, Hebei, China, in 2004 and the Ph.D. degree in materials physics and chemistry from the South China University of Technology, Guangzhou, China, in 2009.

He is currently an Associate Researcher with the State Key Laboratory of Luminescent Materials and Devices, South China University of Technology. His current research interests include metal-oxide TFT and OLED materials and device physics and process.

YU-RONG LIU received the B.S. degree in semiconductor physics from Jiangxi University, Ganzhou, China, in 1991, the M.Sc. degree in condensed physics from Sichuan University, Sichuan, China, in 1996, and the Ph.D. degree in microelectronics and solid-state electronics from the South China University of Technology, Guangzhou, China, in 2007.

He is currently an Associate Professor with the School of Electronic and Information Engineering, South China University of Technology. His current research interests include inorganic/organic thin-film transistors, solar cells, and microsensors.

JUN-BIAO PENG received the Ph.D. degree in physics from the Chinese Academy of Sciences, Beijing, Guangdong, China, in 1993.

He was a Post-Doctoral Researcher with the Korea Institute of Science and Technology, Seoul, South Korea, from 1994 to 1996, and a Visiting Senior Researcher with the Japan Industrial Technology Research Institute, Tokyo, Japan, from 1998 to 2001. He is currently a Professor with the South China University of Technology, and the Dean of the School of Material Science and Engineering.